

## Hydraulic and sedimentary processes causing anastomosing morphology of the upper Columbia River, British Columbia, Canada

Bart Makaske<sup>a,\*</sup>, Derald G. Smith<sup>b</sup>, Henk J.A. Berendsen<sup>a,1</sup>, Arjan G. de Boer<sup>a,2</sup>,  
Marinka F. van Nielen-Kiezebrink<sup>a,3</sup>, Tracey Locking<sup>b</sup>

<sup>a</sup> Department of Physical Geography, Faculty of Geosciences, Utrecht University, P.O. Box 80115, 3508 TC Utrecht, The Netherlands

<sup>b</sup> Department of Geography, University of Calgary, Calgary, Alberta, Canada T2N 1N4

### ARTICLE INFO

#### Article history:

Received 5 January 2009

Received in revised form 22 April 2009

Accepted 23 April 2009

Available online 3 May 2009

#### Keywords:

Anastomosing river

Avulsion

Bedload

Fluvial geomorphology

Sediment transport

Stream power

### ABSTRACT

The upper Columbia River, British Columbia, Canada, shows typical anastomosing morphology – multiple interconnected channels that enclose floodbasins – and lateral channel stability. We analysed field data on hydraulic and sedimentary processes and show that the anastomosing morphology of the upper Columbia River is caused by sediment (bedload) transport inefficiency, in combination with very limited potential for lateral bank erosion because of very low specific stream power ( $\leq 2.3 \text{ W/m}^2$ ) and cohesive silty banks. In a diagram of channel type in relation to flow energy and median grain size of the bed material, data points for the straight upper Columbia River channels cluster separately from the data points for braided and meandering channels. Measurements and calculations indicate that bedload transport in the anastomosing reach of the upper Columbia River decreases downstream. Because of lateral channel stability no lateral storage capacity for bedload is created. Therefore, the surplus of bedload leads to channel bed aggradation, which outpaces levee accretion and causes avulsions because of loss of channel flow capacity. This avulsion mechanism applies only to the main channel of the system, which transports 87% of the water and >90% of the sediment in the cross-valley transect studied. Because of very low sediment transport capacity, the morphological evolution of most secondary channels is slow. Measurements and calculations indicate that much more bedload is sequestered in the relatively steep upper anastomosing reach of the upper Columbia River than in the relatively gentle lower anastomosing reach. With anastomosing morphology and related processes (e.g., crevassing) being best developed in the upper reach, this confirms the notion of upstream rather than downstream control of upper Columbia River anastomosis.

© 2009 Elsevier B.V. All rights reserved.

### 1. Introduction

The anastomosing upper Columbia River, British Columbia, Canada (Fig. 1), is composed of multiple, roughly “straight” channels that are laterally stable. The morphodynamics of this fluvial system are dominated by frequent crevassing – erosive formation of gaps in the natural levee by floodwater – and avulsion (Smith, 1983; Makaske et al., 2002). Straight, laterally stable channels like those of the anastomosing upper Columbia River are an important category of fluvial channels that have received relatively little attention in geomorphological and

hydraulic research. Work in this field has strongly focused on the braided-meandering transition (e.g., Leopold and Wolman, 1957; Carson, 1984; Van den Berg, 1995; Bledsoe and Watson, 2001), while straight channels were often supposed to be rare. Yet “straight” channels – i.e., low to moderately sinuous but laterally stable channels (Makaske, 2001, pp. 156–157) – are very common elements of inland anastomosing river systems (Smith, 1973, 1983, 1986; Makaske, 1998, 2001) and river deltas (Kolb, 1963; Morton and Donaldson, 1978; Makaske, 1998).

Frequent crevassing and avulsion are generally believed to be associated with rapid floodplain aggradation (Makaske, 2001). However, avulsion is not merely a result of (differential) floodplain aggradation, but also of in-channel processes that result in a decrease of the ability of a channel to carry sediment and discharge (see also Jones and Schumm, 1999). Recent papers on the hydraulic and sedimentary processes in the upper Columbia (Tabata and Hickin, 2003; Abbado et al., 2005) addressed the matter of the efficiency of anastomosing channels for transporting water and sediment, and the question of whether anastomosing rivers are equilibrium forms. These studies are responses to an argument made by Nanson and Huang (1999) that some anastomosing rivers are basically fine tuned to transport water and sediment with maximum efficiency across low-gradient plains. This view was contradicted by results reached

\* Corresponding author. Present address: Alterra, Wageningen University and Research Centre, P.O. Box 47, 6700 AA Wageningen, The Netherlands. Tel.: +31 317 481609; fax: +31 317 419000.

E-mail addresses: [bart.makaske@wur.nl](mailto:bart.makaske@wur.nl) (B. Makaske), [dgsmit@ucalgary.ca](mailto:dgsmit@ucalgary.ca) (D.G. Smith), [a.de.boer@archeologie.nl](mailto:a.de.boer@archeologie.nl) (A.G. de Boer), [marinka.van.nielen@rws.nl](mailto:marinka.van.nielen@rws.nl) (M.F. van Nielen-Kiezebrink).

<sup>1</sup> Henk Berendsen passed away on May 14, 2007.

<sup>2</sup> Present address: ADC ArcheoProjecten, P.O. Box 1513, 3800 BM Amersfoort, The Netherlands.

<sup>3</sup> Present address: Rijkswaterstaat-Waterdienst, P.O. Box 17, 8200 AA Lelystad, The Netherlands.

by Tabata and Hickin (2003) and Abbado et al. (2005), which suggested inefficiency of the anastomosing upper Columbia River channels. Points not addressed in these studies, however, are the lateral channel stability of the upper Columbia channels and its role in the formation of the anastomosing system, whereas detailed analysis of in-channel sedimentary processes contributing to anastomosis is also still lacking. Previous work (Smith, 1983; Makaske et al., 2002) demonstrated the long-term lateral stability of the upper Columbia channels and suggested significant bed aggradation in the anastomosing channels.

In this study, in-channel hydraulic and sedimentary processes of the upper Columbia River are examined to better understand its lateral channel stability and mechanisms of crevassing and avulsion. More specifically, in this paper we (i) present stream power and sediment transport data for the straight upper Columbia River channels; (ii) analyse the position of these channels, relative to meandering and braided channels, in an energy-grain size plot; and (iii) carry out a sediment (bedload) budget analysis for two different upper Columbia River reaches to assess bed aggradation rates.

We primarily use field data collected by Makaske (1998) in a cross-valley study transect located roughly halfway along the anastomosing reach of the upper Columbia River, between Radium and Golden, 9 km upstream of Parson, British Columbia (Fig. 1). These data are supplemented by bedload transport measurements carried out by Locking (1983) upstream and downstream of the transect (Fig. 1) and by longitudinal river gradient data of the anastomosing reach collected by Abbado et al. (2005).

**2. Geographical setting and characteristics of the upper Columbia River**

The Columbia River has its source in Columbia Lake and flows northwestward. Major tributaries to the upper Columbia River drain the Purcell Mountains, which flank the Columbia Valley to the SW (Fig. 1). Locally, the Purcell Mountains rise above 3000 m amsl (above

mean sea level) and glaciers surround the highest peaks. Minor creeks drain the lower Kootenay Ranges of the Rocky Mountains on the NE side of the Columbia Valley. These ranges are free of ice with a number of summits close to 2700 m amsl.

The upper Columbia Valley has a humid continental climate with cold winters and warm summers. Mean monthly temperatures on the valley bottom for January and July are  $-10\text{ }^{\circ}\text{C}$  and  $17\text{ }^{\circ}\text{C}$ , respectively. Mean annual precipitation is 490.7 mm at Golden (Meteorological Service of Canada, personal communication, 2002). Higher in the mountains, precipitation is much greater, with the Purcell Mountains being known for deep and prolonged snow covers. At the end of most winters the equivalent of 500 to 750 mm of rain lies over the massif as snowpack (Hare and Thomas, 1974, p. 111).

Above the Nicholson gauging station (Fig. 1), the drainage area of the upper Columbia River is 6660 km<sup>2</sup>, with an annual mean discharge of 107 m<sup>3</sup>/s (data from Water Survey of Canada). Water discharge in the upper Columbia River fluctuates seasonally in response to rainfall and snowmelt, while glacial meltwater constitutes only a minor component of the total discharge. Minimum discharge occurs during the winter – usually in the period from December to March when ice covers the river. Minimum monthly mean discharge is 23.2 m<sup>3</sup>/s in February. In the spring, snowmelt and rain cause a sharp rise and a peak in discharge in June or July (Fig. 2). Maximum monthly mean discharge is 318 m<sup>3</sup>/s in July and bankfull level is exceeded almost yearly.

The upper Columbia River has a narrow floodplain flanked by mountain slopes and tributary valleys from which alluvial fans protrude into the Columbia Valley. The system is laterally restricted (~1.5 km wide), but longitudinally continuous for at least 100 km between Radium and Golden (Fig. 1). Over most of its anastomosing reach, the upper Columbia River consists of a main channel and a variable number of smaller parallel channels. Within the anastomosing reach, the alluvial valley floor has a mean elevation of around 790 m amsl and a generally gentle slope, averaging 11.5 cm/km. The Holocene part of the unconsolidated valley-fill is probably about 20 m thick (Junck, 2009).

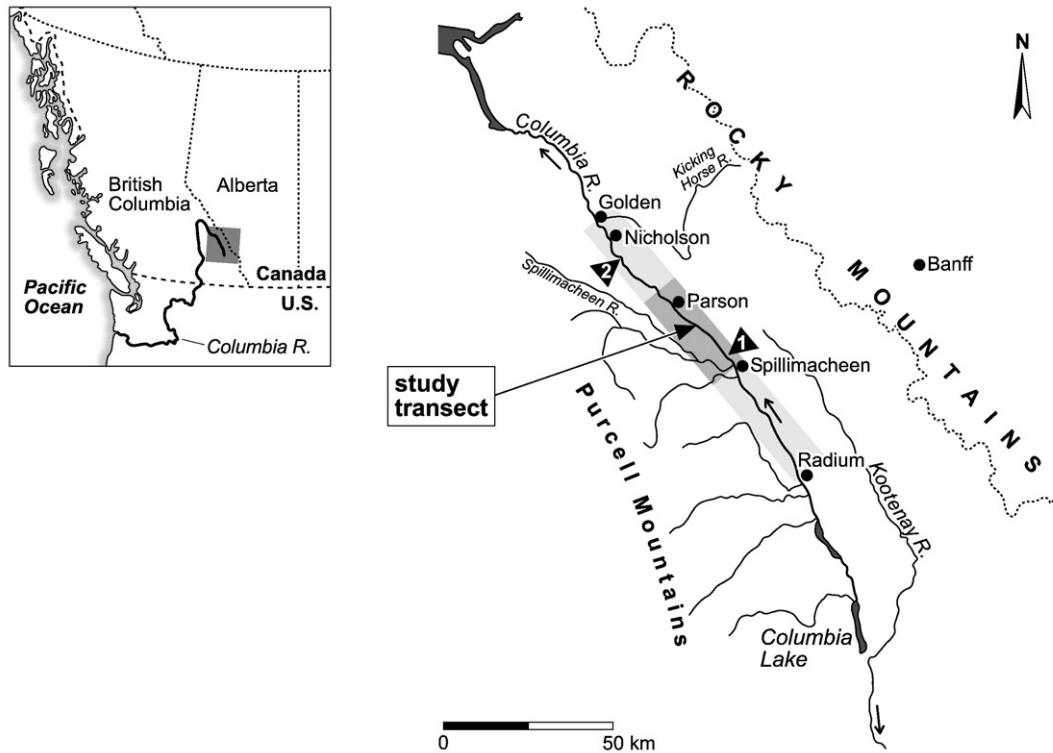


**Fig. 1.** The location of the cross-valley upper Columbia River study transect in SE British Columbia, Canada. The grey zone indicates the anastomosing reach of the upper Columbia River. The dark grey zone indicates the reach shown in Fig. 3. Black triangles indicate the temporary upstream (location 1) and downstream (location 2) gauging stations where hydraulic and bedload transport data were collected by Locking (1983).

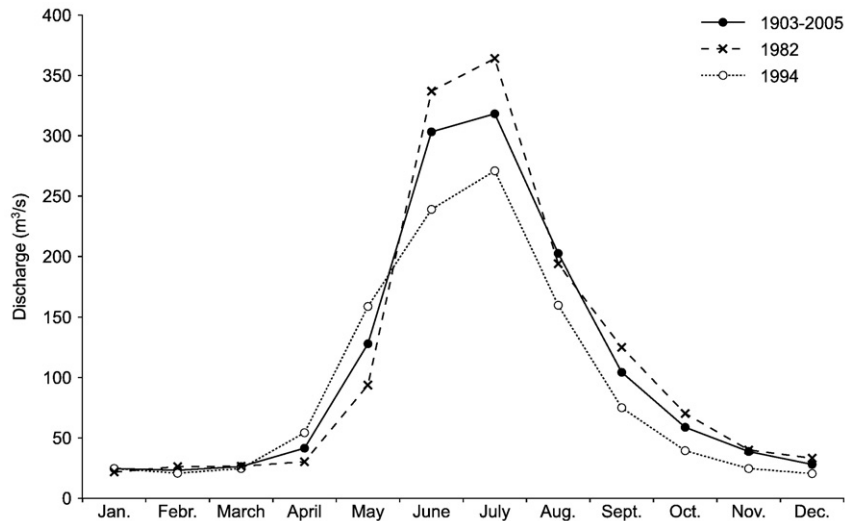


Fig. 2. Mean monthly discharges of the Columbia River at Nicholson, BC, (see Fig. 1 for location) for the period 1903–2005 and for 1982 and 1994 (data from Water Survey of Canada, station 08NA002).

Abbado et al. (2005) distinguished two contrasting anastomosing Columbia River reaches (Fig. 3) downstream of Spillimacheen, where the Spillimacheen River – an important tributary – enters the Columbia Valley. The relatively steep upper reach is characterized by well-developed anastomosis, with three to five parallel channels. A significant break in slope marks the transition to the relatively gentle lower reach in which anastomosis is weakly developed, with typically two to three parallel channels. Abbado et al. (2005) suggested higher aggradation rates in the upper reach as a cause of better developed anastomosis.

### 3. Research site and methods

Fieldwork was carried out in the Columbia Valley from May to July 1994 to enable measurements at discharges near bankfull. The cross-valley transect in which the data were collected is the same as the transect studied sedimentologically and chronologically by Makaske et al. (2002), who demonstrated that the channels in the transect formed by avulsion between ~30 and 3000 years ago and that the channels generally evolved through a consistent pattern of different morphodynamic stages of young widening and deepening channels to old shallowing and narrowing channels. They also reported high lateral facies variability, with clayey and silty floodbasin deposits contrasting with narrow and thick sandy channel fills that indicate long-term lateral channel stability.

A cross-valley transect study enables us to sum measured and calculated water and sediment fluxes to obtain total Columbia River estimates that can be compared with available station data. The studied transect is situated near the transition from the “highly anastomosed” reach upstream and the “weakly anastomosed” reach downstream (Fig. 3), and thereby facilitates a sediment budget calculation for both reaches because sediment transport data have been collected (Locking, 1983) upstream near Spillimacheen and downstream near Nicholson (Fig. 1).

The transect extends across the floodplain from the McKeeman Creek alluvial fan to the opposite valley side, thereby crossing six active channels of variable dimensions (Fig. 4). All studied channels have a low sinuosity index ( $P_{ind} = \text{channel length}/\text{length along channel-belt axis}$ ; Brice, 1964; Makaske, 2001, p. 156) between 1.00 and 1.05 (Table 1) and can thus be classified as straight channels (cf. Makaske, 2001) that have experienced no significant lateral migration. In general, the channels are relatively deep and narrow, with width/depth ratios below 10, but some channels have greater width/depth ratios of about 20 (Table 1). The wet perimeter of the channels typically has a trapezoidal shape. Channel 6

was blocked by a large beaver dam allowing no significant discharge, so hydraulic data were only gathered for channels 1 through 5. In terms of discharge, channel 3 is by far the most dominant (Table 2).

The floodplain topography of the transect was levelled relative to an arbitrary datum, and echo soundings provided data on submerged channel morphology. The echo sounder used provided a vertical resolution of about 2.5 cm and was mounted on an inflatable boat with an outboard motor. Echo soundings were related to land-level data through frequent water stage measurements.

Flow velocity measurements were carried out in the five channels to determine bankfull discharge as a basis for the calculation of stream power and sediment transport. Bankfull stage was defined by the break in slope between the steep channel bank and the flatter surface of the levee. In the case of a difference in elevation between the break in slope for the two banks, the lowest level was chosen. On the basis of five discharge measurements near bankfull stage, stage-discharge graphs were constructed for each channel from which discharge at bankfull stage was interpolated. For each discharge measurement, vertical velocity profiles were measured from the boat, which was attached to a wire guideline stretched across the channel. A small propeller current meter mounted on a finned probe was lowered with a winch. Velocities were measured at 0.25, 0.50, 1.00, 2.00 and 4.00 m (if applicable) above the bottom, and often an additional measurement was carried out near the water surface. Each velocity measurement lasted 100 s. Velocity profiles were measured at breaks in the bed morphology of the channel cross sections. Mean velocity in each vertical profile was calculated from the plotted surface area of the velocity vertical. Spatial integration over the channel cross section yielded total channel discharge. The number of velocity profiles per channel averaged 12 in the main channel and 9 in the smaller channels, and represent the maximum resolution that could be achieved under the ruling field conditions.

Grab samples of bed material were taken with a Van Veen grab sampler (Oele et al., 1983, p. 357). Series of three to seven grab samples were taken twice during the field season in each channel cross section. Sampling locations were roughly evenly distributed over the wet channel perimeter. Laboratory grain size analyses were carried out on 44 grab samples by the standard sieving/pipette method (McManus, 1988).

Channel gradients are needed for the calculation of stream power and sediment transport. The channel gradient – or energy gradient in a channel – can be approximated by the water-surface gradient if steady uniform flow is assumed. We did not succeed in accurately measuring the low channel gradients in this study. Abbado et al. (2005, their Fig. 4) calculated an average channel gradient of 6.8 cm/km for the reach in



which our transect is located, based on many GPS data points. This value is considered the best approximation of the channel gradient of channel 3 (the main channel) in our study. The related valley gradient – accounting for a channel sinuosity of 1.16 – is 7.9 cm/km. Channel gradients of the other channels in the transect were calculated from this valley gradient, taking into account the differences between the direction of maximum valley slope and the directions of the channels on the valley bottom.

As an estimate of the energy available for bank erosion, specific stream power ( $\omega$ ) under bankfull conditions was calculated for each channel, applying  $\omega = \gamma g Q_{bf} S_c / w$  in which  $\gamma$  is the density of water,  $g$  is the acceleration of gravity,  $Q_{bf}$  is bankfull discharge,  $S_c$  is the channel gradient, and  $w$  is the (bankfull) channel width. In order to compare the flow energy and sedimentary characteristics of the Columbia River channels with meandering and braided channels from the literature, the parameter  $S_v \sqrt{Q_{bf}}$  for each channel was plotted against  $D_{50}$  of the bed material in a diagram of [Bledsoe and Watson \(2001\)](#). They analysed a large data set of meandering and braided channels previously published by [Van den Berg \(1995\)](#) and proposed a

logistic regression model to describe the probabilistic (“fuzzy”) nature of the transition from meandering to braiding, thereby extending [Van den Berg’s \(1995\)](#) work on the meandering-braided transition.

Sediment transport capacity at bankfull discharge was assessed for each channel using three different sediment transport equations: (i) the Van Rijn formula ([Van Rijn, 1984a,b](#)), (ii) the modified Van Rijn formula ([Van den Berg and Van Gelder, 1993](#)), and (iii) the [Engelund and Hansen \(1967\)](#) formula. In a test of sediment transport equations, the Van Rijn formula ([Van Rijn, 1984a,b](#)) proved to be a fairly reliable predictor ([Van Rijn, 1993](#)). [Van den Berg and Van Gelder \(1993\)](#), however, showed that at low flow velocities the Van Rijn formula underestimated the transport rates. Under these conditions, the [Engelund and Hansen \(1967\)](#) formula performed better, which is largely a result of the fact that it does not account for critical bed shear stress. Therefore, [Van den Berg and Van Gelder \(1993\)](#) proposed some modifications of the Van Rijn formula, mainly concerning the Shields limit and the near bed reference concentration, which enhanced its predictive power.

[Locking \(1983\)](#) measured discharge and bedload transport during the 1982 flood season near Spillimacheen and Nicholson ([Fig. 1](#)). For



**Fig. 3.** Satellite images of the anastomosing upper Columbia River, between Spillimacheen and a point 6 km downstream of Parson, BC, Canada (see [Fig. 1](#) for location). Images from Google Earth (details in [Fig. 4](#)). The upper Columbia floodplain is flanked by the Kootenay Ranges (NE) and the Purcell Mountains (SW). The Canadian Pacific Railway (CPR) runs along the northeastern edge of the floodplain. Dark colours indicate the forested southwestern valley side. Images taken in the summer flood season with river stage near bankfull and inundated floodbasins. Panels (A) through (D) show successive reaches downstream from the point where the Spillimacheen River joins the upper Columbia, with panels slightly overlapping. (A) and (B) show the “highly anastomosed” reach upstream of the studied transect, which is characterized by three to five parallel channels and channel slopes of up to 21.5 cm/km ([Abbado et al., 2005](#)). Note the pale colour of the floodbasin waters in this reach because of a large supply of sediment-rich water through crevasses. (C) and (D) show the “weakly anastomosed” lower reach, which is characterized by two to three parallel channels and channel slopes of 6.8 cm/km ([Abbado et al., 2005](#)).





Fig. 3 (continued).

the discharge measurements, Locking (1983) broadly followed the procedure outlined above, using a Price AA current meter with two velocity measurements taken at 2/10 and 8/10 depth of each vertical profile (11–15 vertical profiles across the channel). For bedload transport measurements, a Helley-Smith bedload sampler was used for two measurements (15 s each) at each measured vertical velocity profile. At both gauging stations, 10 coupled discharge-bedload transport determinations were carried out in the period June–August 1982 and were used to calculate total bedload fluxes for the 1982 flood season. Application of the Van Rijn (1984a) bedload transport formula to the hydraulic and bedload grain size data collected by Locking (1983) yielded that the Van Rijn formula predicts bedload transport rates that are on average 58 (Spillimacheen station) to 157% (Nicholson station) of the measured rates.

#### 4. Results

Bankfull discharge of the anastomosing system in the transect is  $220 \text{ m}^3/\text{s}$  (Table 2). Considerable differences in mean flow velocity at bankfull discharge exist between the channels (Table 3) and are probably related to differences in hydraulic radius. In channel 4, flow velocity is remarkably high for the small hydraulic radius. In Fig. 5 the measured cross-sectional flow velocity patterns are given for each channel for a stage close to bankfull. The velocity patterns are fairly

symmetrical. Even in channel 5, where the cross section is located just downstream of a bend apex, the thalweg is located in the middle of the channel. Vertical velocity gradients over the flat central portion of the channel beds are much more pronounced than over the sloping banks. Near the channel margins of channels 1, 3, and 5, velocity at the surface is significantly lower than at some depths. This indicates relatively great influence of sidewall roughness because of variable bank morphology, stuck driftwood, and tree branches hanging in the water. In channel 2, rushes growing on the left bank retarded the flow over the full depth.

The low-relief channel bed and the sloping banks are very different in grain size composition (Fig. 6). The bank material is cohesive, with low percentages of clay (~5%), but very high percentages of silt (typically ~50%). The silty material probably originates from the terraces of glaciolacustrine deposits, which flank the Columbia River floodplain in the south. The bed material typically consists of 85–95% sand, with exception of the crevasse channel (channel 2), where the silt and sand contents of the bed material are approximately 40 and 60%, respectively. Lumps of slumped mud, clay pebbles, leaves, and wood were frequently found in the grab samples of the bed material. The bed material of most channels consists of medium sand (Table 4), which is moderately sorted on average (scale of Folk and Ward, 1957). Again, the bed material of channel 2 is different, being characterized by fine, poorly sorted sand.



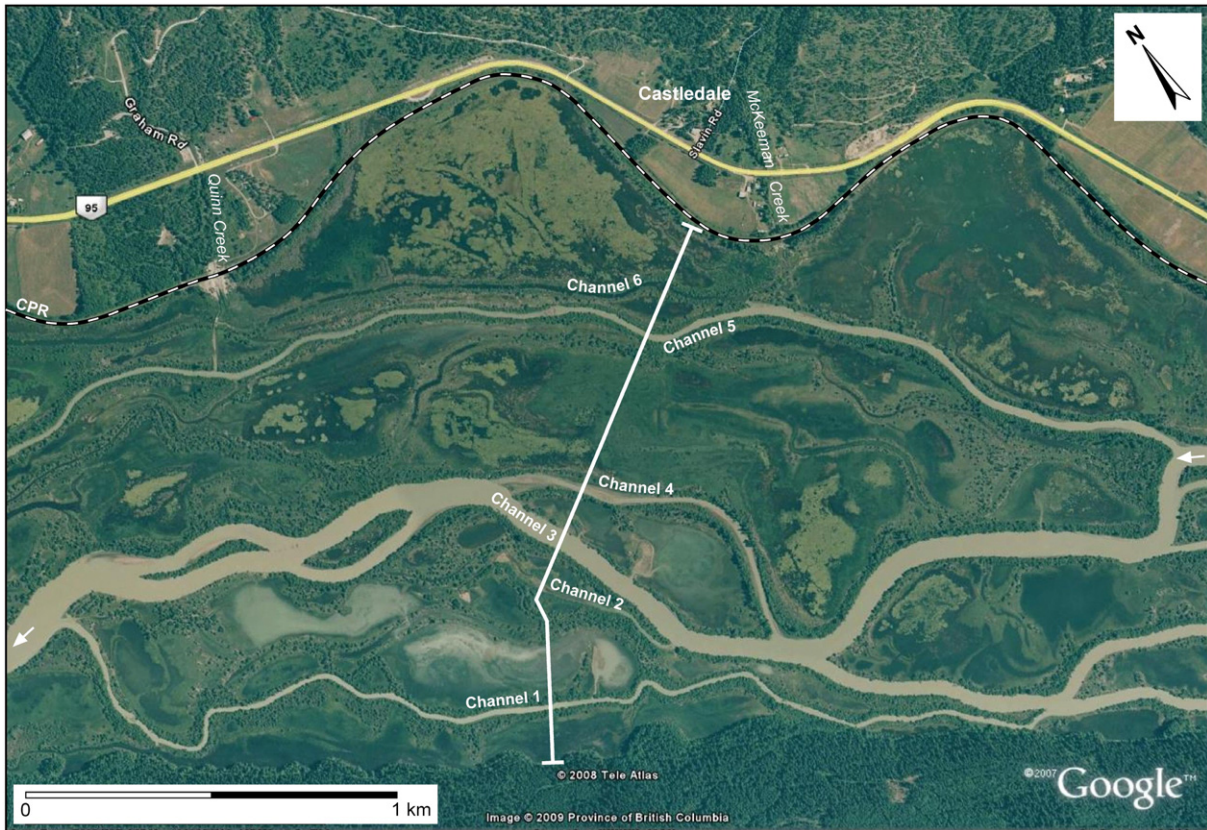


**Fig. 4.** Satellite image of the upper Columbia River floodplain around the studied transect. Flow is from right to left. Image is from Google Earth and taken in the summer flood season, with river stage near bankfull and inundated floodbasins.

In **Table 5**, gradient and specific stream power data for the channels in the transect are listed. The channel gradients vary little as a function of slight differences in sinuosity and channel orientation relative to the direction of maximum valley gradient. All specific stream power values in **Table 5** can be classified as extremely low, when compared to data from the literature (e.g., [Ferguson, 1981](#); [Nanson and Croke, 1992](#)). **Fig. 7** shows that the median grain size of the bed material is finely tuned to specific stream power, which underscores that specific stream power determines present-day sedimentary processes in the upper Columbia channels.

The  $S_v\sqrt{Q_{bf}}$  values for the upper Columbia River channels are below all  $S_v\sqrt{Q_{bf}}$  data plotted by [Bledsoe and Watson \(2001\)](#), which represent predominantly braided and meandering channels (**Fig. 8**). Seemingly, the inactive “straight” upper Columbia River channels plot as a separate class below meandering and braided channels in the diagram, with channel 2 taking the lowest position and channel 3 plotting closest to the meandering channel data points. Two additional data points (6 and 7 in **Fig. 8**) represent straight channels in the upper Inland Niger Delta in central Mali ([Makaske, 1998](#)) – an arid-zone, but perennial, anastomosing

river system. Other additional data points (or data ranges) represent interpreted straight (point 8) and confined meandering (point 9) palaeochannels from the Rhine-Meuse delta ([Makaske and Weerts, 2005](#); [Makaske et al., 2007](#)). The discriminant line between straight and meandering channels in **Fig. 8** is necessarily tentative and in reality may not parallel the meandering-braided transition. Because of the limited straight channel data points (and limited data range), we refrained from a logistic regression analysis (cf. [Bledsoe and Watson, 2001](#)) to define a probabilistic discriminator between straight and meandering channels.

The calculated transport rates (**Table 6**) show that the sediment transport capacity of channel 3 greatly exceeds the capacity of the four other channels together. The highest sediment transport rates are predicted by the modified Van Rijn formula. These are more than twice as high as the prediction by the original Van Rijn formula. The Engelund and Hansen formula predicts slightly higher transport rates for most secondary channels because the critical shear stress is not taken into account. In the smaller channels, the bed shear stress under bankfull conditions was only slightly above the critical shear stress

**Table 1**  
Morphometric characteristics of the studied channels.<sup>a</sup>

	Width (m)	Depth (m)	w/d ratio (-)	P <sub>ind</sub> (-)
Channel 1	19.30	2.12	9.1	1.04
Channel 2	24.80	1.08	23.0	1.00
Channel 3	56.03	5.85	9.6	1.04
Channel 4	20.70	1.04	19.9	1.04
Channel 5	18.63	3.17	5.9	1.05
Channel 6	18.00	2.90	6.2	1.04

<sup>a</sup> Bankfull width; maximum depth relative to bankfull level; w/d = width/depth; P<sub>ind</sub> = sinuosity index.

**Table 2**  
Bankfull discharge.<sup>a</sup>

	Q <sub>bf,1</sub> (m <sup>3</sup> /s)	Q <sub>bf,2</sub> (m <sup>3</sup> /s)	(%)
Channel 1	9.5	8.4	3.8
Channel 2	2.4	2.8	1.3
Channel 3	193.5	192.0	87.1
Channel 4	5.4	6.1	2.8
Channel 5	14.8	11.1	5.0
Total		220.4	100.0

<sup>a</sup> Q<sub>bf,1</sub> = bankfull discharge for each individual channel; Q<sub>bf,2</sub> = discharge when the entire anastomosing system is approximately at bankfull stage.

**Table 3**  
Flow velocities and flow dimensions at bankfull discharge.<sup>a</sup>

	$u_{\text{mean}}$ (m/s)	$R$ (m)	$h_{\text{mean}}$ (m)	$A$ (m <sup>2</sup> )
Channel 1	0.32	1.4	1.54	29.8
Channel 2	0.15	0.6	0.65	16.0
Channel 3	0.79	4.1	4.37	244.8
Channel 4	0.35	0.8	0.75	15.5
Channel 5	0.40	1.8	1.99	37.0

<sup>a</sup>  $u_{\text{mean}}$  = mean flow velocity in flow area;  $R$  = hydraulic radius;  $h_{\text{mean}}$  = mean channel depth;  $A$  = flow area.

required to initiate motion of the bed material. In channel 2, shear stress did not exceed the critical level, which was confirmed by bed observations before and after peak discharge, showing that the mud drape on the sandy bed had remained largely intact. Consequently, sediment transport in the smaller channels of the anastomosing system is almost negligible (Table 6), and only stages well above bankfull can bring about substantial sediment transport in channels other than the main channel.

An important limitation is that all sediment transport formulae only predict the transport capacity for the locally available sandy bed material. Great quantities of finer material are transported as washload, unrelated to the transport capacity as calculated with a sediment transport formula. The Van Rijn formula and the modified Van Rijn formula make a distinction between bedload and suspended load.

Predicted bedload for the main channel is 20 to 43% of the predicted total load. Measurements of sediment concentrations by Locking (1983) upstream and downstream of the present study transect indicate bedload to be 11% of the total load. In these measurements, however, measured suspended load included washload. The measured values therefore were much greater than the predicted quantities.

When the measured bedload transport data from Locking (1983) are combined with the calculated bedload transport data from the present study transect, sediment budgets of the upper and lower anastomosing reaches of the upper Columbia can be estimated. The upper anastomosing reach between Locking's measurement site near Spillimacheen (Fig. 1) and the present study site is 15 km long (main channel distance) and is characterized by an ~10-km-long, relatively steep section with a channel slope of 21.5 cm/km (Abbado et al., 2005). The lower anastomosing reach between the present study site and Locking's measurement site near Nicholson (Fig. 1) is 35 km long (main channel distance) with a fairly constant average channel slope of 6.8 cm/km. Based on the hydraulic and sediment transport data from Locking (1983), bedload input into the upper anastomosing reach during bankfull discharge (~220 m<sup>3</sup>/s) is estimated at 7.1 kg/s. At the same discharge, bedload transport at the study site is 1.9 kg/s, according to our calculations. However, because the Van Rijn formula predicts upper Columbia River bedload transport rates between 58 and 157% of the measured values, real bedload transport at the study site may be in the range of 1.2 to 3.3 kg/s. Near Nicholson, bedload output from the lower anastomosing reach at bankfull discharge (~220 m<sup>3</sup>/s) is estimated at 0.6 kg/s (Fig. 9).

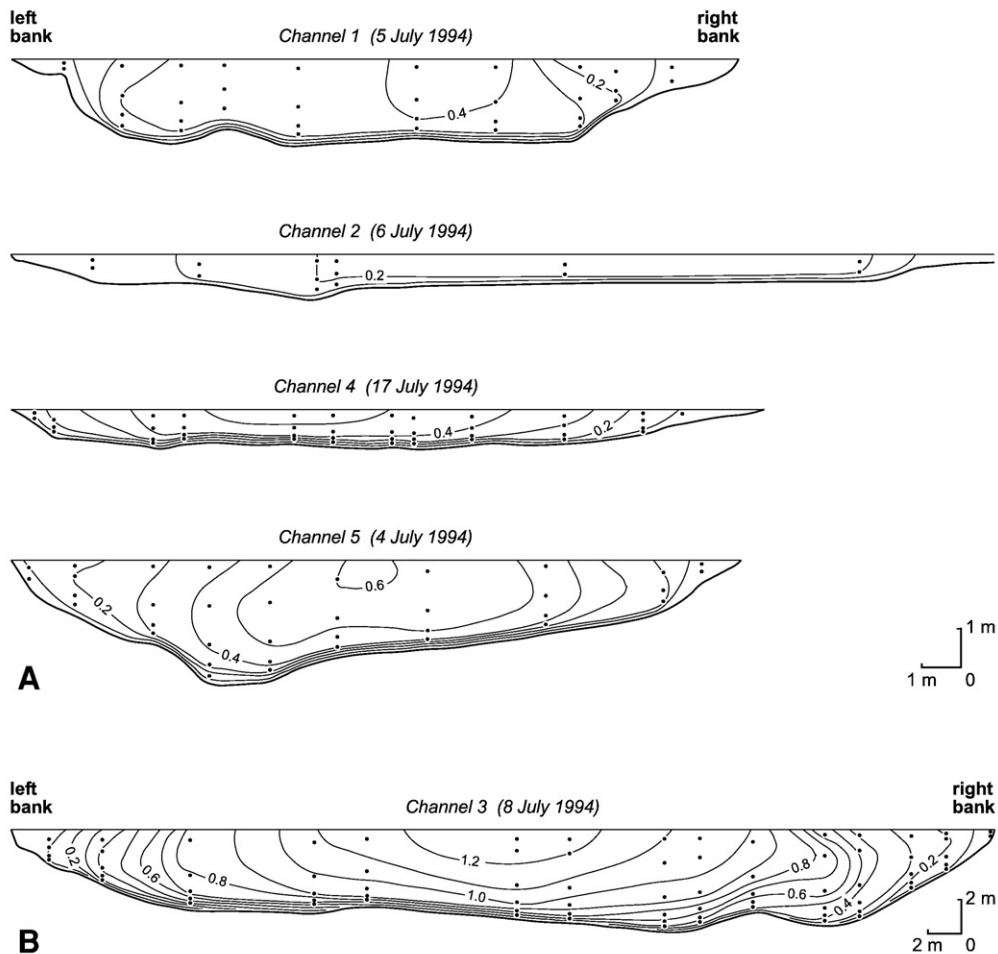


**Fig. 5.** Measured cross-sectional flow velocity (in m/s) patterns near bankfull discharge in (A) channels 1, 2, 4, and 5 and (B) channel 3 (note the different scale of this cross section). The black dots indicate flow velocity measurements. Flow is away from the observer.

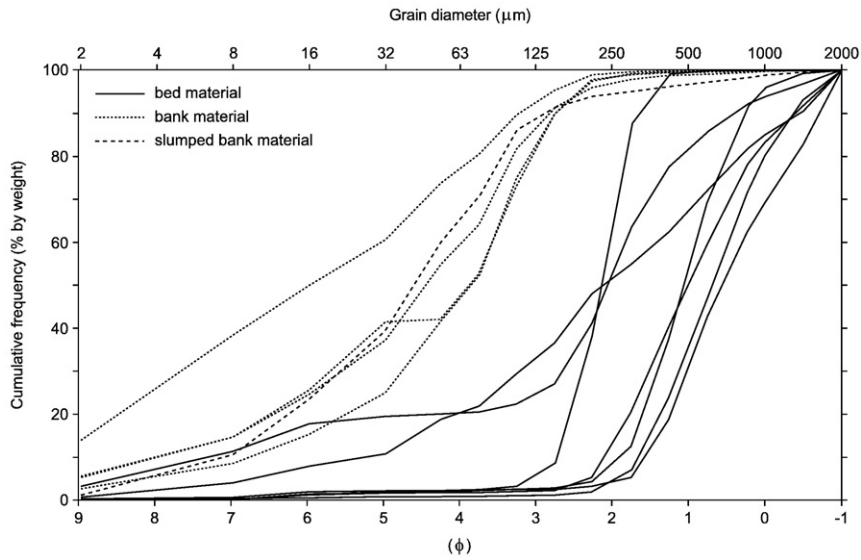


Fig. 6. Grain size distributions of bed and bank material of the main channel (channel 3).

Thus, at bankfull discharge, 58 to 91% of the bedload trapped between Spillimacheen and Nicholson is sequestered in the upper anastomosing reach, and 9 to 42% is sequestered in the lower anastomosing reach (Fig. 9). Assuming that (i) these proportions are representative for the entire flood season, i.e., bankfull discharge is dominant discharge; (ii) bedload sequestration in the anastomosing reach largely occurs in the summer flood season, as indicated by Locking’s measurements showing limited bedload surplus at stages well below bankfull; and (iii) the 1982 flood season roughly represents the average flood season, we can estimate the total amounts of bedload that are trapped annually in the upper and lower anastomosing reaches (Fig. 9). Because the 1982 flood was above average (Fig. 2), we might slightly overestimate bedload sequestration. However, this overestimation is probably compensated for by the fact that we neglect bedload sequestration out of the flood season.

**5. Lateral channel stability and bed aggradation causing anastomosis**

The specific stream power of the studied upper Columbia River channels (Table 5) is within the ranges mentioned in the literature for straight, laterally stable, channels. Nanson and Croke (1992) suggested an upper boundary of 10 W/m<sup>2</sup> for low-energy river systems with laterally stable channels. Ferguson (1981) mentioned a range of 1 to 60 W/m<sup>2</sup> – with a median of about 15 W/m<sup>2</sup> – for (laterally) inactive channels. The low specific stream power of the upper Columbia River channels indicates that little energy is available for lateral erosion of the cohesive silty banks (Fig. 6), which explains the straight channel morphology.

**Table 4**  
Grain size of the bed material.<sup>a</sup>

	Mean $D_{50}$ (µm)	Mean $D_{90}$ (µm)	$\sigma_s$ (-)
Channel 1	282	680	1.86
Channel 2	107	323	2.29
Channel 3	431	1077	2.01
Channel 4	253	405	1.54
Channel 5	301	970	2.18

<sup>a</sup>  $D_{50}$ ,  $D_{90}$  = grain sizes in a distribution for which 50% and 90% by weight, respectively, are finer;  $\sigma_s = 1/2 (D_{50}/D_{16} + D_{84}/D_{50})$  representing the gradation of the bed material (based on means of  $D_{16}$ ,  $D_{50}$  and  $D_{84}$ ) with  $D_{50}$  as given earlier and  $D_{16}$  and  $D_{84}$  representing grain sizes in a distribution for which 16% and 84% by weight, respectively, are finer.

In our analysis of channel morphology, we followed the approach of Van den Berg (1995), Bledsoe and Watson (2001), and Van den Berg and Bledsoe (2003). Their work, however, has been criticised by Lewin and Brewer (2001, 2003) who claimed that the analysis based on energy-grain size plots (such as Fig. 8) insufficiently appreciates a range of important factors influencing river channel patterns. As an example of the latter they state that “the limited migration of anastomosing channels may well in part reflect low bankfull stream power, but bank cohesion seems to be important...” (Lewin and Brewer, 2003, p. 341). Our analysis shows that – although bank cohesion undoubtedly contributes to the lateral stability of anastomosing upper Columbia River channels – the factors “energy” and “bed grain size” seem sufficient to discriminate these inactive “straight” channels from meandering and braided ones.

In meandering rivers, bedload is stored in point bars, and hence, storage capacity is largely determined by the rate of lateral channel migration. In the upper Columbia River – where lateral migration of channels is negligible and point bars are absent – storage of bedload takes place on the channel bed. For the channels in the study transect, we estimate that channel shallowing occurs if bed aggradation exceeds the average natural levee growth rate of 1.65 mm/year (Fig. 10). This study shows negligible sediment transport rates in secondary channels (Table 6), rendering bed aggradation rates in excess of 1.65 mm/year highly unlikely for these channels. Calculated sediment transport rates suggest that only in the main channel (channel 3) can bed aggradation exceed 1.65 mm/year.

Our sediment budget calculations indicate an annual bed aggradation in the main channel of 13.3 to 20.9 mm in the upper anastomosing reach based on Fig. 9, a main channel bed area of 1,500,000 m<sup>2</sup> (15 km long, 100 m wide), and a sediment density of 1770 kg/m<sup>3</sup> (Locking, 1983). Even if bed aggradation is substantially overrated and levee accretion is substantially underrated, bed

**Table 5**  
Channel gradients and stream power.<sup>a</sup>

	$S_c$ (cm/km)	$\omega$ (W/m <sup>2</sup> )
Channel 1	7.8	0.38
Channel 2	7.4	0.07
Channel 3	6.8	2.30
Channel 4	7.6	0.19
Channel 5	7.4	0.58

<sup>a</sup>  $S_c$  = channel gradient;  $\omega$  = specific stream power at bankfull discharge.



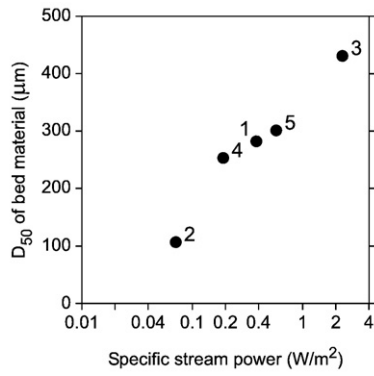


**Fig. 7.** Plot of median grain size (mean of multiple samples) of the channel bed material against the specific stream power at bankfull discharge. Numbers of data points refer to channel numbers.

aggradation very likely outpaces levee accretion in this reach (Fig. 11). Levee accretion in the upper anastomosing reach may exceed the 1.65 mm/year that was inferred for the present study site, but is

**Table 6**  
Total sediment transport (bedload + suspended load) at bankfull discharge according to three equations.

	Eng.-Hansen	Van Rijn	Mod. Van Rijn
	$Q_t$ (g/s)	$Q_t$ (g/s)	$Q_t$ (g/s)
Channel 1	126	0	16
Channel 2	24	0	0
Channel 3	5877	4411	9824
Channel 4	75	14	62
Channel 5	236	43	312

unlikely to be much greater than 3.7 to 4.7 mm/year, representing the maximum measured levee accretion during single flood seasons (Makaske et al., 2002; Filgueira-Rivera et al., 2007). For the lower anastomosing reach, main channel bed (35 km long, 100 m wide) aggradation rates between 0.9 and 4.1 mm/year can be calculated. With a long-term levee aggradation rate of 1.65 mm/year channel shallowing is still likely to occur but at a much slower rate than in the upper anastomosing reach (Fig. 11). Locally, some channel widening

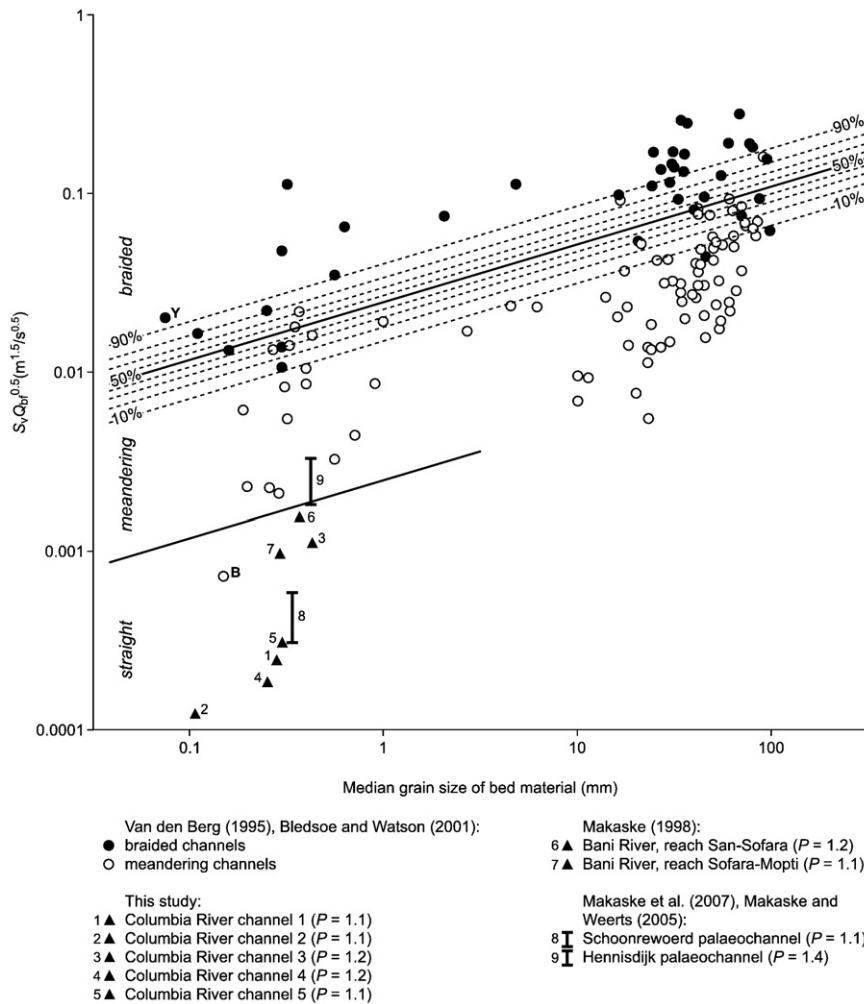


**Fig. 8.** Diagram of channel type in relation to grain size and the flow energy parameter  $S_v \sqrt{Q_{bf}}$  ( $S_v$  is valley slope and  $Q_{bf}$  is bankfull discharge), with a discriminator based on logistic regression analysis indicating the probability of braiding (Bledsoe and Watson, 2001 with data from Van den Berg, 1995). Data points B (Barwon River) and Y (Yellow River) added from Van den Berg's original data set, but not used by Bledsoe and Watson (2001) in the logistic regression analysis. Data on straight channels from the present study are plotted along with some additional data from the literature. Channels with a sinuosity ( $P$ ) > 1.3 were classified as meandering by Van den Berg (1995) and Bledsoe and Watson (2001). Note that some of these "meandering" channels are in fact laterally stable, having a low sinuosity index ( $P_{ind}$  = channel length/length along channel-belt axis; Brice, 1964; Makaske, 2001, p. 156). This means that the sinuosity of these channels is not the result of lateral migration. An example is the Barwon River (data point B) (Taylor and Woodyer, 1978), which plots near the straight channels from this study. A preliminary discriminant line is drawn between the populations of meandering and straight ( $P \leq 1.3$  and  $P_{ind} < 1.3$ ) channels.

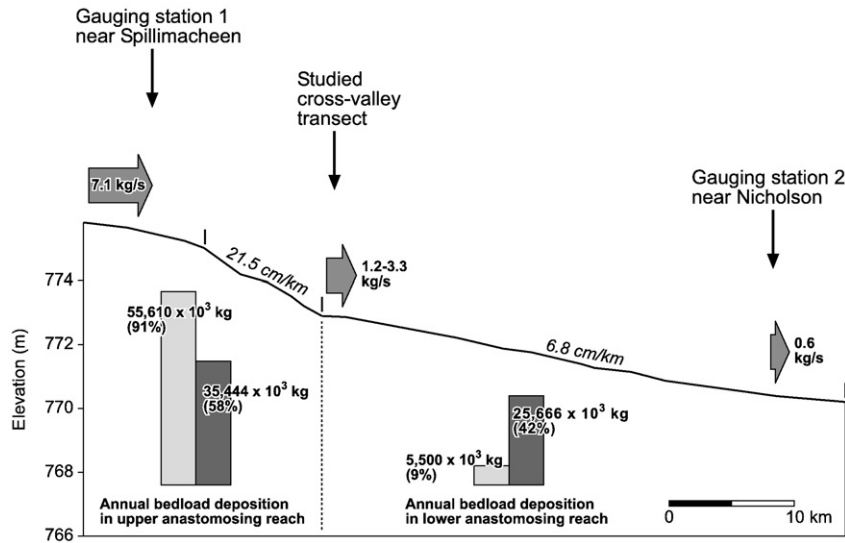


**Fig. 9.** Longitudinal profile of the upper Columbia River main channel between locations 1 and 2 in Fig. 1 – showing a relatively steep upper reach and a relatively gentle lower reach – and bedload fluxes at bankfull discharge (~220 m<sup>3</sup>/s). Amounts and proportions of bedload (relative to total bedload stored in anastomosing reach) stored annually in the upper and lower anastomosing reaches are also given. Light grey bars represent scenario with maximum difference between sediment storage in upper and lower anastomosing reach (based on maximum calculated sediment throughput in transect), dark grey bars represent scenario with minimum difference between sediment storage in upper and lower anastomosing reach (based on maximum calculated sediment throughput in transect). The channel gradients indicated were measured by Abbado et al. (2005) over the period 13–15 October 2000 when river discharge was ~55 m<sup>3</sup>/s. These low stage water surface gradients may slightly deviate from high stage water surface gradients.

by slumping of river banks may partly compensate for the loss of flow area caused by bed aggradation. Rapid bank retreat, however, will destroy the levee and induce crevassing and avulsion.

Hence, the main channel is most liable to avulsions, many secondary channels being virtually inactive morphologically. Exceptions are young secondary channels formed by avulsion, which may rapidly develop (widening and deepening) because of significant gradient/energy advantage. Older secondary channels exist for very long periods, their morphological evolution in general being determined by trapping of fine suspended and washload in bank vegetation leading to very slow channel narrowing (Makaske et al., 2002, their Fig. 14). Log jams may speed up abandonment of secondary channels. Some secondary channels receive ample bedload and coarse suspended load and totally fill up with sand because of specific conditions near the channel entrance. Channel 4, for example, is very shallow and – unlike other

secondary channels – totally fills up with sandy bedload because its entrance is located on the inside of a bend in the main channel (Fig. 4). Because of this configuration, this channel receives a relatively large proportion of the coarse load from the main channel, as shown by general bifurcation modelling by Kleinhans et al. (2008), which demonstrated that meandering river bifurcations are inherently unstable because of asymmetric division of water and sediment associated with morphological evolution in meander bends. Usually, within a geologically short period (a few decades to centuries), one branch will be plugged by sediment, whereas the other branch receives most of the discharge. Only very special conditions permitted longer bifurcation stability. This modelling result explains the observation (Makaske, 2001) that anastomosing rivers that are composed of individual meandering channels, such as the Owens and King Rivers (Schumm et al., 1996), are much less common than anastomosing rivers consisting of straight channels, like the upper Columbia River.

Anastomosis of the upper Columbia River initially was understood to result from a downstream control – i.e., a rising base level caused by aggrading cross-valley alluvial fans (Smith, 1983). This idea was challenged by Abbado et al. (2005), who showed that anastomosis is most pronounced in the upper reach between Spillimacheen and our study transect, where much sediment is introduced by the Spillimacheen River (Fig. 3). Our results confirm their idea of an upstream (excessive bedload supply) rather than a downstream cause (base level rise) of upper Columbia River anastomosis. That both upstream and downstream controls can give rise to frequent avulsions in low-energy, multiple channel systems was demonstrated in the Rhine-Meuse delta by Stouthamer and Berendsen (2001) and Gouw and Erkens (2007).

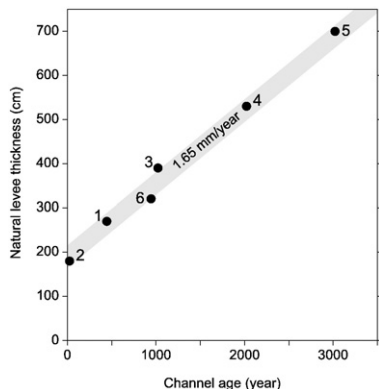


**Fig. 10.** Plot of natural levee thickness (including basal crevasse splay deposits) against the age of the associated upper Columbia River channel (data from Makaske et al., 2002, representing the same cross-valley transect as in the present study). Numbers of data points refer to channel numbers. This graph indicates that after initial rapid crevasse splay deposition of ~2 m – associated with avulsive channel formation – natural levee aggradation approaches a nearly constant rate of 1.65 mm/year for all channels. This value may seem low relative to the long-term average upper Columbia floodplain sedimentation rate of 1.75 mm/year (Makaske et al., 2002), but the latter includes rapid crevasse splay sedimentation, which importantly contributes to overall long-term floodplain sedimentation.

**6. Conclusions**

Results from this study indicate that anastomosing morphology of the upper Columbia River is generated from the inability of the river to transport its entire bedload. An important circumstance also, is that the upper Columbia channels have no ability to migrate laterally because of low stream power and erosion-resistant bank material. In a diagram of channel type in relation to flow energy and median grain size of the bed material, data points for the straight upper Columbia



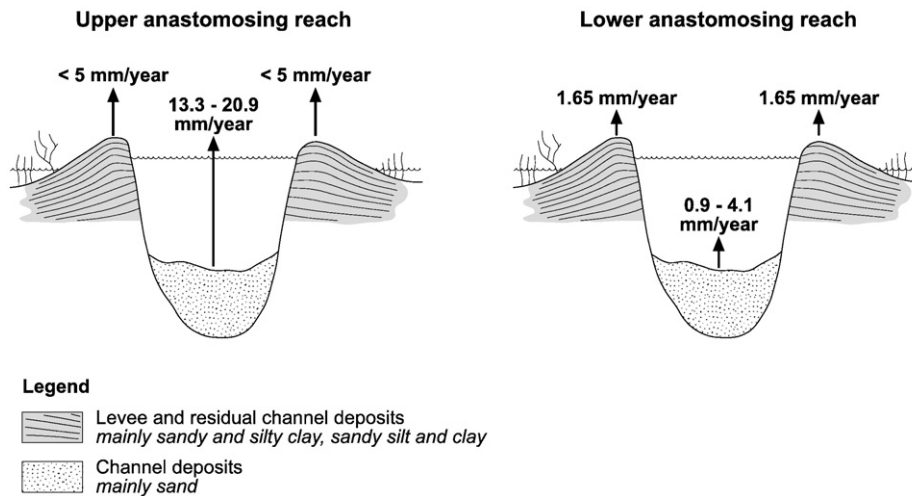


Fig. 11. Bed and levee accretion rates for the upper Columbia River main channel in the upper and lower anastomosing reaches (Figs. 3 and 9). Vertical exaggeration approximately 10 $\times$ .

River channels cluster separately from the data points for braided and meandering channels. Because of lateral channel stability, no lateral storage capacity for the surplus of bedload supplied to the Columbia River main channel is created. Much of it is stored on the channel bed, leading to gradual decrease in flow capacity, increased overbank flooding and sedimentation, crevassing, and cutting of new channels on the floodplain.

In a number of publications (e.g., Slingerland and Smith, 1998; Törnqvist and Bridge, 2002), avulsion is described as a result of floodplain accretion, creating steep cross-levee gradients that provide an energy advantage for floodwaters relative to channel flow. Results from this study point to bed aggradation as the primary mechanism of avulsion in the upper Columbia River. This study quantitatively demonstrates that bed aggradation in the upper Columbia main channel outpaces levee accretion, whereas the morphological evolution of most secondary channels is slow because of very low sediment transport capacity. The development of steep cross-levee gradients is probably not an important driver of avulsions in the upper Columbia River, because valley width is limited and floodbasins are small with water levels usually close to channel water levels. In other words, in our case avulsion seems rather “pushed” by bed aggradation than “pulled” by gradient advantage.

Our calculations demonstrate that bed aggradation in the upper anastomosing reach of the upper Columbia River where anastomosis is particularly well developed, is much faster than in the lower reach, and thereby confirm the idea (Abbado et al., 2005) of an upstream (excessive bedload supply) rather than a downstream cause (base level rise) of upper Columbia River anastomosis. This study shows that — next to ample bedload supply — anastomosis is favoured by a relatively low stream power limiting lateral channel migration and creation of lateral storage capacity for excess bedload. In general, low stream powers may result from low slopes caused by rising base levels; so in this indirect sense, rising base levels may contribute to anastomosis — for example in near-coastal settings subjected to relative sea level rise. For the upper Columbia River, the present role of downstream control is uncertain because aggradation of downstream cross-valley alluvial fans determining local base level seems to be insignificant today, with incised fan channels and stable fan surfaces.

## Acknowledgements

This paper is dedicated to co-author Henk Berendsen, who initiated this research many years ago and extensively commented on drafts of this paper until shortly before he passed away. Maarten Kleinhans is thanked for sharing his insights into bifurcation morphodynamics. We

are grateful to Stephen Tooth for his useful comments on a draft of this paper. This paper benefitted from constructive reviews by Nicholas Pinter and an anonymous referee. Financial support for carrying out fieldwork and analyses was granted by Utrecht University and the Natural Sciences and Engineering Research Council (NSERC) of Canada.

## References

- Abbado, D., Slingerland, R., Smith, N.D., 2005. Origin of anastomosis in the upper Columbia River, British Columbia, Canada. In: Blum, M.D., Marriot, S.B., Leclair, S.M. (Eds.), *Fluvial Sedimentology VII*. Special Publication of the International Association of Sedimentologists, vol. 35. Blackwell, Oxford, UK, pp. 3–15.
- Bledsoe, B.P., Watson, C.C., 2001. Logistic analysis of channel pattern thresholds: meandering, braiding, and incising. *Geomorphology* 38, 281–300.
- Brice, J.C., 1964. Channel patterns and terraces of the Loup Rivers in Nebraska. U.S. Geological Survey Professional Paper 422-D, Washington, DC.
- Carson, M.A., 1984. The meandering-braided river threshold: a reappraisal. *Journal of Hydrology* 73, 315–334.
- Engelund, F., Hansen, E., 1967. *A Monograph on Sediment Transport in Alluvial Streams*. Teknisk Forlag, Copenhagen, Denmark.
- Ferguson, R.I., 1981. Channel form and channel changes. In: Lewin, J. (Ed.), *British Rivers*. Allen & Unwin, London, pp. 90–211.
- Filgueira-Rivera, M., Smith, N.D., Slingerland, R.L., 2007. Controls on natural levee development in the Columbia River, British Columbia, Canada. *Sedimentology* 54, 905–919.
- Folk, R.L., Ward, W.C., 1957. Brazos River bar: a study in the significance of grain size parameters. *Journal of Sedimentary Petrology* 27, 3–26.
- Gouw, M.J.P., Erkens, G., 2007. Architecture of the Holocene Rhine-Meuse delta (the Netherlands); a result of changing external controls. *Netherlands Journal of Geosciences - Geologie en Mijnbouw* 86, 23–54.
- Hare, F.K., Thomas, M.K., 1974. *Climate Canada*. Wiley, Toronto.
- Jones, L.S., Schumm, S.A., 1999. Causes of avulsion: an overview. In: Smith, N.D., Rogers, J. (Eds.), *Fluvial Sedimentology VI*. Special Publication of the International Association of Sedimentologists, vol. 28. Blackwell, Oxford, UK, pp. 171–178.
- Junck, M.B., 2009. Sub-surface Imaging of Cross-valley Alluvial Fans: using Ground Penetrating Radar (GPR) and Electric Resistivity Ground Imaging (ERGI) to determine Holocene Sedimentation Thicknesses in Trunk Valleys. M.Sc. thesis, Department of Geography, University of Calgary, Alberta, Canada.
- Kleinhans, M.G., Jagers, H.R.A., Mosselman, E., Sloff, C.J., 2008. Bifurcation dynamics and avulsion duration in meandering rivers by one-dimensional and three-dimensional models. *Water Resources Research* 44, W08454.
- Kolb, C.R., 1963. Sediments forming the bed and banks of the lower Mississippi River. *Sedimentology* 2, 227–234.
- Leopold, L.B., Wolman, M.G., 1957. *River channel patterns: braided, meandering and straight*. U.S. Geological Survey Professional Paper 282-B, Washington, DC.
- Lewin, J., Brewer, P.A., 2001. Predicting channel patterns. *Geomorphology* 40, 329–330.
- Lewin, J., Brewer, P.A., 2003. Reply to Van den Berg and Bledsoe’s comment on Lewin and Brewer (2001) “Predicting channel patterns.” *Geomorphology* 40, 329–339.
- Locking, T., 1983. *Hydrology and Sediment Transport in an Anastomosing Reach of the Upper Columbia River*. B.C. M.Sc. thesis, Department of Geography, University of Calgary, Alberta, Canada.
- Makaske, B., 1998. *Anastomosing Rivers; Forms, Processes and Sediments*. Nederlandse Geografische Studies 249. Koninklijk Nederlands Aardrijkskundig Genootschap/Faculteit Ruimtelijke Wetenschappen, Universiteit Utrecht, Utrecht, The Netherlands.

- Makaske, B., 2001. Anastomosing rivers: a review of their classification, origin and sedimentary products. *Earth-Science Reviews* 53, 149–196.
- Makaske, B., Weerts, H.J.T., 2005. Muddy lateral accretion and low stream power in a subrecent confined channel belt, Rhine-Meuse delta, central Netherlands. *Sedimentology* 52, 651–668.
- Makaske, B., Smith, D.G., Berendsen, H.J.A., 2002. Avulsions, channel evolution and floodplain sedimentation rates of the anastomosing upper Columbia River, British Columbia, Canada. *Sedimentology* 49, 1049–1071.
- Makaske, B., Berendsen, H.J.A., Van Ree, M.H.M., 2007. Middle Holocene avulsion-belt deposits in the central Rhine-Meuse delta, The Netherlands. *Journal of Sedimentary Research* 77, 110–123.
- McManus, J., 1988. Grain size determination and interpretation. In: Tucker, M.E. (Ed.), *Techniques in Sedimentology*. Blackwell, Oxford, UK, pp. 63–85.
- Morton, R.A., Donaldson, A.C., 1978. Hydrology, morphology, and sedimentology of the Guadalupe fluvial-deltaic system. *Geological Society of America Bulletin* 89, 1030–1036.
- Nanson, G.C., Croke, J.C., 1992. A genetic classification of floodplains. *Geomorphology* 4, 459–486.
- Nanson, G.C., Huang, H.Q., 1999. Anabranching rivers: divided efficiency leading to fluvial diversity. In: Miller, A., Gupta, A. (Eds.), *Varieties of Fluvial Form*. Wiley, New York, pp. 477–494.
- Oele, E., Apon, W., Fischer, M.M., Hoogendoorn, R., Mesdag, C.S., De Mulder, E.F.J., Overzee, B., Sesören, A., Westerhoff, W.E., 1983. Surveying The Netherlands: sampling techniques, maps and their application. *Geologie en Mijnbouw* 62, 355–372.
- Schumm, S.A., Erskine, W.D., Tilleard, J.W., 1996. Morphology, hydrology, and evolution of the anastomosing Ovens and King Rivers, Victoria, Australia. *Geological Society of America Bulletin* 108, 1212–1224.
- Slingerland, R., Smith, N.D., 1998. Necessary conditions for a meandering-river avulsion. *Geology* 26, 435–438.
- Smith, D.G., 1973. Aggradation of the Alexandra–North Saskatchewan River, Banff Park, Alberta. In: Morisawa, M. (Ed.), *Fluvial Geomorphology*. Proceedings of the 4th Annual Geomorphology Symposia series, Binghamton, NY, September 27–28, 1973. State University of New York, Binghamton, pp. 201–219.
- Smith, D.G., 1983. Anastomosed fluvial deposits: modern examples from western Canada. In: Collinson, J., Lewin, J. (Eds.), *Modern and Ancient Fluvial Systems*. Special Publication of the International Association of Sedimentologists, vol. 6. Blackwell, Oxford, UK, pp. 155–168.
- Smith, D.G., 1986. Anastomosing river deposits, sedimentation rates and basin subsidence, Magdalena River, northwestern Colombia, South America. *Sedimentary Geology* 46, 177–196.
- Stouthamer, E., Berendsen, H.J.A., 2001. Avulsion frequency, avulsion duration, and interavulsion period of Holocene channel belts in the Rhine-Meuse delta, The Netherlands. *Journal of Sedimentary Research* 71, 589–598.
- Tabata, K.K., Hickin, E.J., 2003. Interchannel hydraulic geometry and hydraulic efficiency of the anastomosing Columbia River, southeastern British Columbia, Canada. *Earth Surface Processes and Landforms* 28, 837–852.
- Taylor, G., Woodyer, K.D., 1978. Bank deposition in suspended load streams. In: Miall, A.D. (Ed.), *Fluvial Sedimentology*. Canadian Society of Petroleum Geologists Memoir, vol. 5. Canadian Society of Petroleum Geologists, Calgary, p. 257–275.
- Törnqvist, T.E., Bridge, J.S., 2002. Spatial variation of overbank aggradation rate and its influence on avulsion frequency. *Sedimentology* 49, 891–905.
- Van den Berg, J.H., 1995. Prediction of alluvial channel pattern of perennial rivers. *Geomorphology* 12, 259–279.
- Van den Berg, J.H., Bledsoe, B.P., 2003. Comment on Lewin and Brewer (2001): "predicting channel patterns." *Geomorphology* 40, 329–339. *Geomorphology* 53, 333–337.
- Van den Berg, J.H., Van Gelder, A., 1993. Prediction of suspended bed material transport in flows over silt and very fine sand. *Water Resources Research* 29, 1393–1404.
- Van Rijn, L.C., 1984a. Sediment transport, part I: bed load transport. *Journal of Hydraulic Engineering* 110, 1431–1456.
- Van Rijn, L.C., 1984b. Sediment transport, part II: suspended load transport. *Journal of Hydraulic Engineering* 110, 1613–1641.
- Van Rijn, L.C., 1993. *Principles of Sediment Transport in Rivers, Estuaries and Coastal Seas*. Aqua Publications, Amsterdam, The Netherlands.